Preparation of Microcellular Poly(ethylene-*co*-octene) Rubber Foam with Supercritical Carbon Dioxide

Wentao Zhai,[1] Siu N. Leung,[1] Lilac Wang,[1] Hani E. Naguib,[1,2] Chul B. Park[1]

[1]*Microcellular Plastics Manufacturing Laboratory, Department of Mechanical and Industrial Engineering, University of Toronto, Toronto, Ontario M5S 3G8, Canada*
[2]*Department of Materials Science and Engineering, University of Toronto, Toronto, Ontario M5S 3G8, Canada*

Received 1 May 2009; accepted 21 October 2009
DOI 10.1002/app.31640
Published online 7 January 2010 in Wiley InterScience (www.interscience.wiley.com).

ABSTRACT: In the past 3 decades, there has been great advancement in the preparation of microcellular thermoplastic polymer foams. However, little attention has been paid to thermoplastic elastomers. In this study, microcellular poly(ethylene-*co*-octene) (PEOc) rubber foams with a cell density of 2.9×10^{10} cells/cm^3 and a cell size of 1.9 μm were successfully prepared with carbon dioxide as the physical blowing agent with a batch foaming process. The microcellular PEOc foams exhibited a well-defined, closed-cell structure, a uniform cell size distribution, and the formation of unfoamed skin at low foaming temperatures. Their difference from thermoplastic foam was from obvious volume recovery in the atmosphere because of the elasticity of the polymer matrix. We investigated the effect of the molecular weight on the cell growth process by changing the foaming conditions, and two important effect factors on the cell growth, that is, the polymer matrix modulus/melt viscoelastic properties and gas diffusion coefficient, were assessed. With increasing molecular weight, the matrix modulus and melt viscosity tended to increase, whereas the gas solubility and diffusion coefficient decreased. The increase in the matrix modulus and melt viscosity tended to decrease the cell size and stabilize the cell structure at high foaming temperatures, whereas the increase in the gas diffusion coefficient facilitated cell growth at the beginning and limited cell growth because most of the gas diffused out of the polymer matrix during the long foaming times or at high foaming temperatures.
 J Appl Polym Sci 116: 1994–2004, 2010

Key words: blowing agents; elastomers; microcellular foam; polyolefins

INTRODUCTION

Since the invention of microcellular plastics,[1] the microcellular foaming of polymers has been broadly investigated, and various types of microcellular foams have been produced by various processes, such as batch foaming,[2–4] extrusion,[5–8] and injection molding.[9,10] Various studies have revealed that microcellular foams have the properties of high impact strength,[11–13] high toughness,[14,15] high thermal stability,[16] low dielectric constant,[17] and so on. Even though there has been great success in producing microcellular foams, to our knowledge, most of these studies have focused on thermoplastic polymers, and little attention has been given to thermoplastic elastomers (TPEs).[18–20]

TPEs are a new class of materials that exhibit the properties of conventional thermoset rubbers yet can be processed with thermoplastic processing equipment. Therefore, they bridge the gap between conventional vulcanized rubber and thermoplastics. The majority of TPEs demonstrate heterophase morphologies; that is, they have hard and soft domains.[21] Generally speaking, the hard domains provide tensile strength and normal service temperatures and undergo molecular relaxation at elevated/degraded temperatures. Thus, they allow the materials to flow/solidify. On the other hand, the soft domains give the material its elastomeric characteristics. The unique properties of TPEs render wide use in automotives, construction, appliances, medicine, and electronics.

Poly(ethylene-*co*-octene) (PEOc) is a type of TPE, which is produced by Dow Chemical with a recently developed group-IV-transition-metal-based postmetallocene catalyst.[22] These copolymers exhibit high molecular weights, relatively narrow molecular weight distributions, and unique chain microstructures.[23] These features make the new copolymers excellent vehicles for fundamental studies of structure–property relationships in ethylene copolymers. The origin of the elasticity of PEOc has been well studied[22–24] and originates from the specific crystal structure of PEOc, that is, the fringed micellar

Correspondence to: C. B. Park (park@mie.utoronto.ca).
Contract grant sponsors: AUTO21 Network of Centers of Excellence, Government of Ontario.

TABLE I
Characteristics of the PEOc Foams

Sample	Octene content (%)	Density (g/cm^3)	M_w (g/mol)	M_n (g/mol)	M_w/M_n	Melting point (°C)	Crystallinity (%)	MFR
EG8100	38	0.87	179,700	103,600	1.7	44.6/62.0	6.6	1
EG8200	38	0.87	122,300	65,700	1.8	40.6/63.0	9.7	5
EG8400	40	0.87	82,900	39,900	2.0	42.4/67.5	11.5	30

MFR = melt flow rate; M_n = number-average molecular weight; M_w = weight-average molecular weight.

crystal because, the crystallizable sequence is inadequate in length to allow the chains to fold into lamellar crystals.[23] This type of crystal morphology is far from perfect in comparison to the lamellar crystal structure of thermoplastic polymers.[22] Therefore, it is expected to affect gas solubility, gas distribution in the polymer matrix, and gas diffusion behavior and thereby affect cell nucleation and growth during the PEOc foaming process. Meanwhile, the change in elasticity is an important issue before and after PEOc foaming. Both of these supplied us with motivation to investigate the foaming behavior of PEOc.

In this study, the foaming behavior of PEOc was studied by a temperature-rising process using carbon dioxide (CO_2) as a physical blowing agent. The comparisons of the foaming behaviors between TPE and thermoplastics were carried out from different perspectives, that is, from the perspectives of expansion behavior, cell morphology, and skin characteristics. Three types of PEOc samples with different molecular weights but the same density and similar melting behaviors were selected. Different foaming conditions were applied to show the effect of molecular weight on the microcellular foaming behavior. Considering that PEOc tends to foam during the pressure quenching, we paid more attention to the possible factors that would affect the cell growth process, such as the polymer matrix modulus/melt viscoelastic properties and gas diffusion coefficient. Consequently, in this study, we tried to establish a relationship between the molecular weight and the foaming behavior of PEOc.

EXPERIMENTAL

Materials and sample preparation

Three types of metallocene-catalyzed copolymers of ethylene and 1-octene (PEOc), that is, Engage 8100 (EG8100), Engage 8200 (EG8200), and Engage 8400 (EG8400), were provided by Dow Chemical (Midland, MI). The characteristics of the PEOc studied, such as octane content and melt flow rate, were supplied by Dow Chemical and are shown in Table I. CO_2 with a purity of 99.5% (Linde gas) was used as the physical blowing agent in all of the experiments.

Specimens with thicknesses of 1 and 1.8 mm were prepared by compression molding of the PEOc resins at 150°C. All specimens were disc shaped and had various diameters for different measurements, that is, 25 mm for dynamic rheological measurements and 10 mm for microcellular foaming.

Gas solubility and diffusion coefficient measurements

The PEOc sheets were enclosed in a high-pressure vessel at 25°C. The vessel was flushed with low-pressure CO_2 for about 3 min; we then increased the pressure to 13.8 MPa and saturated the sheets for 15 h. After a rapid quench of pressure, the samples were removed from the vessel and transferred, within a 1-min interval, to a digital balance (sensitivity = 0.1 mg) to record the amount of mass loss as a function of time. The mass uptake of CO_2 in the high-pressure vessel was calculated by linear extrapolation of the initial stage of the desorption curve of CO_2. The desorption diffusion coefficient (D_d) of polymers is calculated as follows[25]:

$$\frac{M_d}{M_\infty} = -\frac{4}{l}\sqrt{\frac{D_d t_d}{\pi}} \quad (1)$$

where M_d is the measured percentage weight loss at the desorption time (t_d), M_∞ is the saturated sorption amount, and l is the original unfoamed thickness.

Batch foaming

The basic process of polymer saturation with CO_2 was the same as that of the gas sorption measurement. After saturation for 15 h to ensure equilibrium sorption of CO_2, the samples underwent a rapid quench of pressure. Then, they were removed from the vessel and transferred, within a 1-min interval, to a water bath kept at a fixed temperature. The samples were foamed in the water bath for 10 s unless otherwise indicated and then quenched in cold water. PEOc tended to foam as the pressure quenched. The samples were further foamed in the water bath with the aim to control the cell morphology of the polymer foam. When the fixed foaming time was gone, the foamed sample was removed from the water bath, and then, it was put on a paper

in the atmosphere. The thickness of the foamed sample was measured with a caliper three times regularly from 1 min to 72 h. The average thickness was used in the final results.

Analysis

The melting temperature was determined with a Q2000 (TA Instruments, USA) that was calibrated with indium. All measurements were carried out with a heating rate of 10°C/min over a temperature range from 30 to 200°C in a dry nitrogen environment. The crystallinity was calculated from the integration of the melting peak of the first heating and with the heat of fusion of 100% crystalline PE (i.e., 290 J/g).[22]

Dynamic rheological measurements were carried out on a strain-controlled ARES rheometer (TA Instruments) with 25-mm parallel-plate geometry and a 1-mm sample gap. Dynamic shear measurements were taken with frequencies from 0.01 to 70 rad/s at temperatures of 150, 170, and 190°C, with strain values determined with a stress sweep to lie within the linear viscoelastic regions. We carried out dynamic temperature sweep tests by cooling the samples from 190 to 40°C at a rate of 5°C/min and then heating the samples back to 190°C at a rate of 5°C/min. All dynamic temperature sweep tests were measured at a strain of 1%.

The morphologies of the foamed samples were observed with a JEOL JMS 6060 (Japan) scanning electron microscope (SEM). The samples were freeze-fractured in liquid nitrogen and sputter-coated with platinum. The cell size and cell density were determined from the SEM micrographs. We calculated the cell diameter by averaging the sizes of at least 100 cells in the SEM micrographs. The cell density and the number of cells per cubic centimeter of unfoamed polymer were determined from eq. (2):

$$N_0 = \left[\frac{nM^2}{A}\right]^{3/2} \phi \tag{2}$$

where N_0 is the cell density, n is number of cells in the SEM micrograph, M is the magnification factor, A is the area of the micrograph (cm^2), and ϕ is the volume expansion ratio of the polymer foam, which was calculated by eq. (3):

$$\phi = \frac{\rho}{\rho_f} \tag{3}$$

where ρ and ρ_f are the mass densities of the samples before and after foaming, respectively, which were measured via the water displacement method in accordance with ASTM D 792.

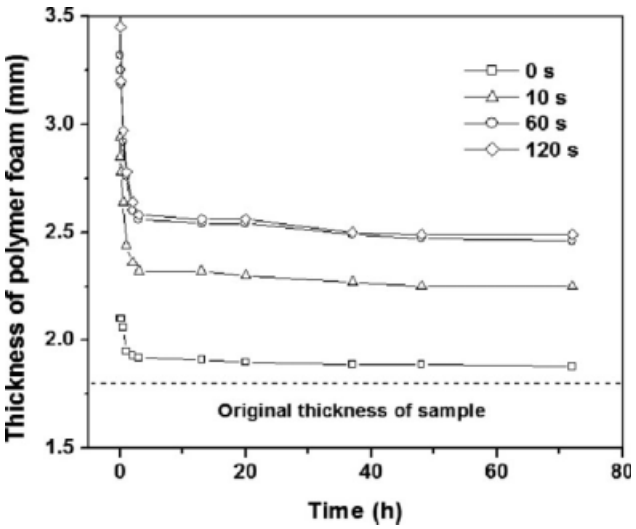

Figure 1 Change in the thickness of the PEOc foams with time in the atmosphere. EG8100 samples were foamed at 50°C for 0, 10, 60, and 120 s after saturation at 13.8 MPa and 25°C and then were exposed to the atmosphere for different times.

RESULTS AND DISCUSSION

PEOc tended to foam as the pressure quenched after CO_2 saturation at 13.8 MPa and 25°C because of its very low melting point and crystallinity. In this study, the depressurization followed by heating was carried out to investigate the foaming behavior of the PEOc rubber.

Expansion behaviors of the PEOc rubbers

PEOc (EG8100) was saturated with CO_2 under 13.8 MPa and at 25°C and then was foamed at 50°C for various times. An obvious volume expansion of the polymer foam in the water bath was observed. However, after the foamed sample was removed from the water bath, the volume of polymer foam tended to decrease in the atmosphere. Figure 1 shows the change in the thickness of the polymer foams with time in the atmosphere. The PEOc foams had initial thicknesses of 2.10, 2.94, 3.32, and 3.54 mm at corresponding foaming times of 0, 10, 60, and 120 s. After their removal from the water bath for 3 h, their thicknesses decreased rapidly to 1.92, 2.32, 2.56, and 2.58 mm, respectively. When the foams were left in the atmosphere for a longer time, further reductions in their thicknesses were observed. The magnitude of decrease in thickness reduced gradually and ceased after 48 h. Eventually, the thicknesses of the foams were 1.88, 2.25, 2.46, and 2.49 mm, respectively. The PEOc foams obtained at various foaming times had different thickness recovery abilities, and longer foaming times resulted in the attainment of more significant increases in their final thicknesses.

This type of expansion behavior of the PEOc rubber foam, which was attributed to the elasticity of the PEOc rubber, is absent in thermoplastic polymer foams. It was well established that the crystallizable ethylene sequences in PEOc can be incorporated into different crystals to form a network with fringed micellar crystals serving as the multifunctional junctions.[23] These physical networks provide the structural basis for the elasticity of TPEs. When gas bubbles form and grow during the polymer foaming process, the matrix tends to stretch. One can fix the elongated shape for a thermoplastic polymer by decreasing the temperature to induce glass transition[26] or crystallization.[27] However, the low glass-transition temperature and crystallinity in TPE suppress the anchor of the extended deformation; therefore, partial recovery tends to occur in the polymer matrix. As shown in Figure 1, the thickness recovery was very quick initially, and a larger recovery was observed for the more deformed sample. Nevertheless, the deformation of the polymer matrix could not be recovered fully after polymer foaming. This was attributed to the rearrangements of crystallites caused by the chain detachment from the crystal surface and its attachment to a neighboring crystal,[23,24] which resulted in permanent deformation.

Cell morphology and formation of the foam skin

PEOc was saturated with CO_2 under 13.8 MPa and then foamed at 50°C for 60 s. Figure 2 shows the cell morphology of the foam under two different magnifications. The foam had a well-defined, closed-cell structure and a uniform cell size distribution. The cell density and cell size were 2.9×10^{10} cells/cm^3 and 1.9 μm, respectively, under these conditions. This indicated the successful preparation of the microcellular foam in the PEOc sample.

The preparation of a microcellular foam with a cell size equal to 1.9 μm and a high cell density is not easy for pure polymers, even with the batch foaming method. Uncommon methods, that is, controlled polymer foaming[28,29] and the selection of polymers with high glass-transition temperatures,[30] are often applied to achieve this purpose. For PEOc, however, in this study, we demonstrated that it was easier to produce a microcellular foam compared with other thermoplastics with the aforementioned characteristics under mild foaming conditions. We speculated that with the existence of crystallites in the polymer matrix, pre-existing gas cavities existed at the interface between the crystalline and the amorphous regions. The expansion of nucleated bubbles near these interfacial regions generated biaxial stretching and thereby generated shear/extensional fields within these local regions.[31,32] Such stress fields reduced the local pressure or even generated a negative pressure in the polymer matrix. As a result, the free energy barrier to nucleate new cells or the critical radius for cell nucleation decreased significantly, which resulted in the expansion of more preexisting gas cavities and, thereby, the increase in the final cell density. In the case of PEOc, the high elasticity and/or residual stress within the matrix was believed to further promote the accumulation of local stress and enhance the stress-induced nucleation.

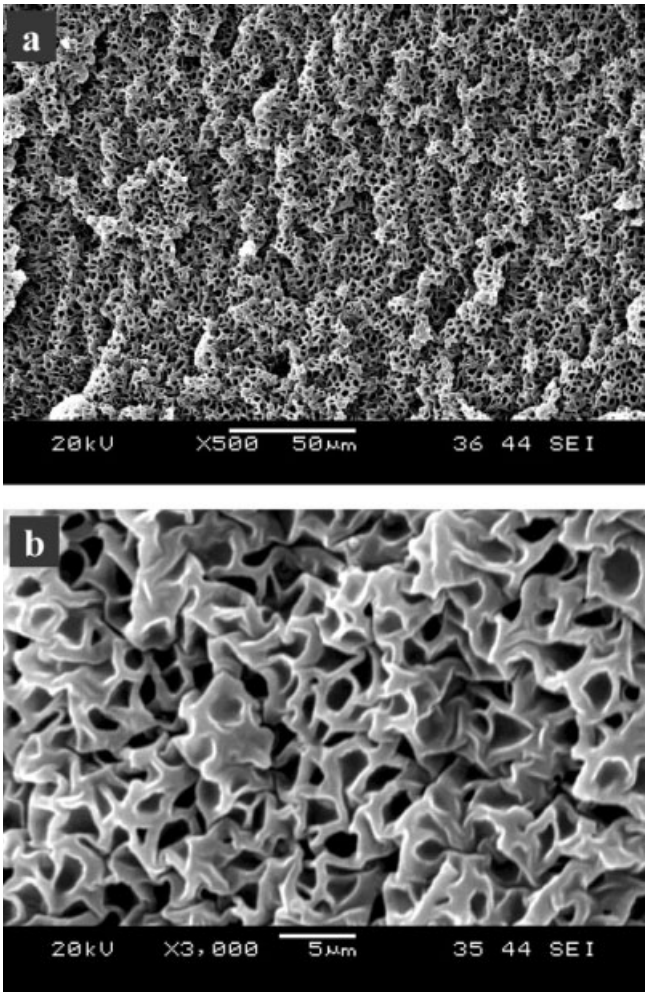

Figure 2 Cell morphology of the EG8100 foam at two different magnifications. The sample was saturated at 13.8 MPa and 25°C and then foamed at 50°C for 60 s.

The uniform cell size distribution indicated two important pieces of information about the foaming PEOc, that is, the effect of the crystal structure on the cell nucleation and when cell nucleation occurred. It is well accepted that for a thermoplastic polymer, the presence of crystal structure tends to affect the cell morphology of foam from two aspects during the batch foaming process. First, the crystal regions may serve as heterogeneous nucleation sites to enhance cell nucleation because of the lower free energy barrier to nucleate a cell at the phase interface.[33–36] Second, the crystal regions may lead to

nonuniform cell nucleation because the gas does not dissolve in the crystallites.[37,38] The presence of a uniform cell size distribution in the PEOc foam indicated that the crystal structure did not induce nonuniform cell nucleation during the PEOc foaming process. A similar phenomenon has been broadly reported for crystalline thermoplastic polymer foams and was attributed to the low crystallinities of the polymers.[38] This explanation seemed suitable for PEOc because its crystallinity was very low, that is, about 10%. However, the crystal structure of the PEOc rubber was fringed micelles, which is imperfect in comparison to the lamellar crystal of thermoplastic polymers.[23,24] This suggests that CO_2 may have dissolved in the crystal regions of PEOc and may have affected the cell nucleation behavior. More detailed studies are needed to elucidate this mechanism.

According to these results, the nucleation step of PEOc foaming occurred during the depressurization. This means that the dissolved gas plasticized the PEOc matrix, and the pressure drop itself gave enough thermodynamic instability to induce cell nucleation, and the polymer was soft enough to allow cell growth. In the subsequent foaming process in the water bath, no obvious further cell nucleation occurred, at least in the foam center, as a uniform cell size distribution was observed in these regions. This hypothesis is further verified by the relationship between the foaming time and cell density in the next section.

The formation of an unfoamed skin is very common in thermoplastic polymer foams prepared with a physical blowing agent. This is often attributed to the short diffusion distance for the gas located in the skin layer,[39,40] which results in no nucleation in those regions because of the increased energy barrier of cell nucleation. An unfoamed skin was also observed in the PEOc foam prepared at a foaming temperature of 30°C, as shown in Figure 3(a), where the skin was 41.7 μm, which was 25 times larger than the cell size in the foam center. This phenomenon indicated that the gas took only the time of half the cell diameter distance, but diffusion had already taken place and caused the loss of most of the gas in a 25-fold length. This means that the cells were not nucleated quickly or might have been nucleated but could not grow because the polymer matrix was stiff at a lower gas concentration. With an increase in the foaming temperature to 70°C, as shown in Figure 3(b2), the unfoamed skin was absent. Furthermore, the closed cell had a large cell size of about 20 μm. Considering the much higher diffusion rate at the higher temperature, cell nucleation was expected to occur in those unfoamed skins during pressure quenching. Otherwise, the foamed samples tended to form a thicker skin at a higher temperature. According to these results, therefore, the cell nucleation should have occurred in the foam skin regardless of the foaming temperatures. The key point was whether the nuclei could grow, which was governed by the critical radii for cell nucleation at those local areas. It seemed that the temperature did not further induce new cell nucleation in the foam center because of the uniform cell size distribution in those regions. A rough surface was observed in the PEOc foam [shown in Fig. 3(b2)], which resulted from the presence of a large cell structure near the foam surface. Interestingly, there was a much stretched structure in the foam surface [shown in Fig. 3(b3)], which possibly resulted from the surface extension due to the initial foam expansion and the following foam shrinkage.

Effect of the molecular weight on the foaming behavior of the PEOc rubber

Three types of PEOc with different molecular weights but the same density and similar melting behaviors were selected to investigate the effect of the molecular weight on the foaming behavior of PEOc. Considering that there was no further cell nucleation occurrence in the water bath, we gave most of our attention to the cell growth process. In the following section, the material parameters governing the cell growth process, that is, the melt viscoelastic properties, polymer matrix modulus, and CO_2 diffusion coefficient and solubility, are discussed first. Then, these factors are used to analyze the relationship between the molecular weight and the foaming behavior of PEOc.

Melt viscoelastic properties and matrix modulus of PEOc

Figure 4 shows the complex viscosity (η^*) of PEOc at various frequencies and a temperature range between 150 and 190°C. The Newtonian plateau at low frequencies was reached for EG8400 at all three testing temperatures and for EG8200 at 190°C. No obvious Newtonian plateau was observed in EG8100 in the frequency range studied. Compared to EG8400, EG8100 and EG8200 exhibited increased viscosity and shear thinning, which were expectably attributed to their higher molecular weights.

A dynamic temperature sweep was carried out to show the temperature dependencies of η^* and storage modulus (G') for three PEOc samples. Because of the obvious time dependency of the polymer crystallization/melting, PEOc exhibited obvious differences in both η^* and G' at temperatures of about 40–75°C between the heating and cooling sweep processes. We believe that the heating sweep supplied more information in this study because the polymer

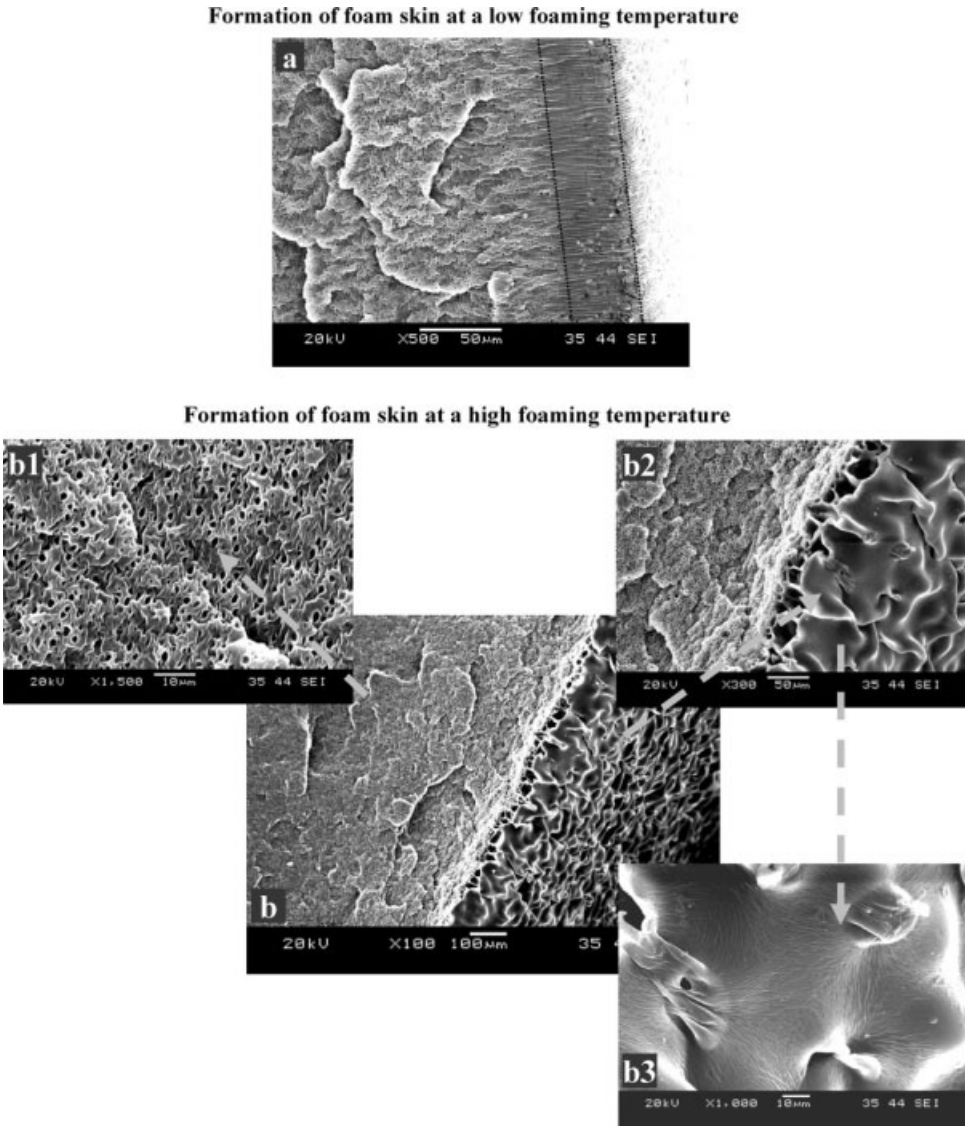

Figure 3 Formation of an unfoamed skin at (a) the low temperature of 30°C and (b) the high temperature of 70°C. EG8100 was saturated at 13.8 MPa and 25°C and then foamed for 10 s at the aforementioned temperatures.

was performed with solid-state foaming. Figure 5 illustrates the temperature dependences of η* and G' for PEOc during the temperature-rising sweep process. G' and η* decreased gradually when the temperature increased between 40 and 60°C. Above 60°C, G' and η* decreased very quickly, as a result of the crystallites melting. At higher temperatures, the decreased magnitudes of G' and η* decreased again until the temperature reached 190°C. G' and η* of EG8100 and EG8200 were higher at 75–190°C and exhibited less temperature dependency compared to that of EG8400. These results indicate that PEOc exhibited increased modulus and melt viscosity with increasing molecular weight, which facilitated the stabilization of cell structure at high foaming temperatures. The three PEOc samples exhibited almost the same G' and η* at 40–60°C, where the crystal regions were not melted completely, in accordance with the DSC results.

Gas solubility and diffusion coefficient measurements

Gas solubility and diffusivity are also important parameters in determining the cell growth and foam expansion. Gas solubility governs the amount of gas that can be used for cell growth, and gas diffusivity affects the growth rates of gas bubbles. In this study, CO_2 solubility in PEOc was measured with a commonly accepted gravimetric method.[28] However, because of the PEOc tendency to foam as the pressure quenched, the gas diffusion was affected by the presence of the cell structure; thus, the obtained data was not accurate.[26] Nevertheless, it should have

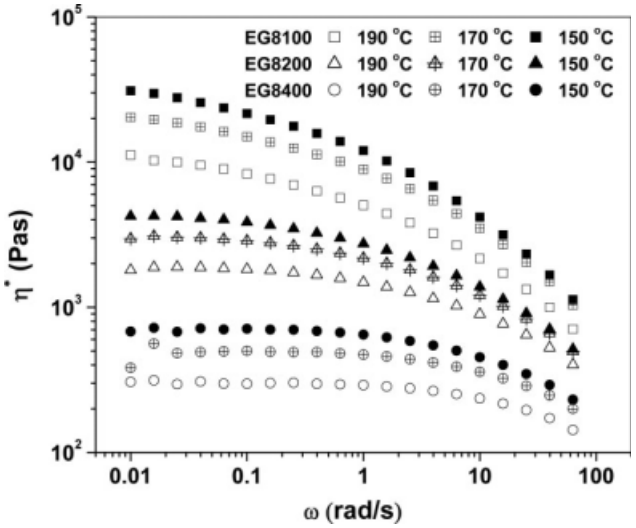

Figure 4 η* versus the angular frequency (ω) for PEOc at 150, 170, and 190°C.

supplied a qualitative tendency. Table II shows the CO_2 solubility and diffusion coefficient values in PEOc. EG8200 exhibited a slightly higher CO_2 solubility and CO_2 diffusivity than EG8100, that is, 13.6 versus 12.3% and 6.15×10^{-10} versus 4.12×10^{-10} m^2/s, respectively, at 25°C. With a further reduction in molecular weight, EG8400 showed a much higher CO_2 solubility of 20.7% and a diffusion coefficient of 1.49×10^{-9} m^2/s, that is, 3.6 times higher than EG8100. These results indicate that the decrease in molecular weight tended to increase CO_2 sorption and diffusion in PEOc. Similarly to EVA,[18] the PEOc rubbers exhibited a relatively high diffusion coefficient, on the order of 10^{-10} to 10^{-9} m^2/s at room temperature, which was 1–2 orders of magnitude higher than that of thermoplastic polymers[41] because of the large free volume in TPEs.[42]

Effect of the molecular weight on the cell growth process

As mentioned previously, the foamed PEOc tended to shrink in the atmosphere. To eliminate any residual stress, the foamed PEOc were exposed to the atmosphere for 2 weeks before we measured the foam density. Figure 6 shows the effects of the foaming time and temperature on the expansion ratio of the PEOc foams. The expansion ratio for the EG8100 foam quickly increased in the initial 30 s, and then, it continued to increase, but at a lower rate, afterward up to 120 s with increasing foaming time. This indicated that the EG8100 foam expanded persistently during the entire foaming process in the water bath. The expansion behavior of the EG8200 foam was similar to that of the EG8100 foam, except that its expansion ratio was slightly higher during 0–60 s and quickly decreased at 120 s. The EG8400 foam

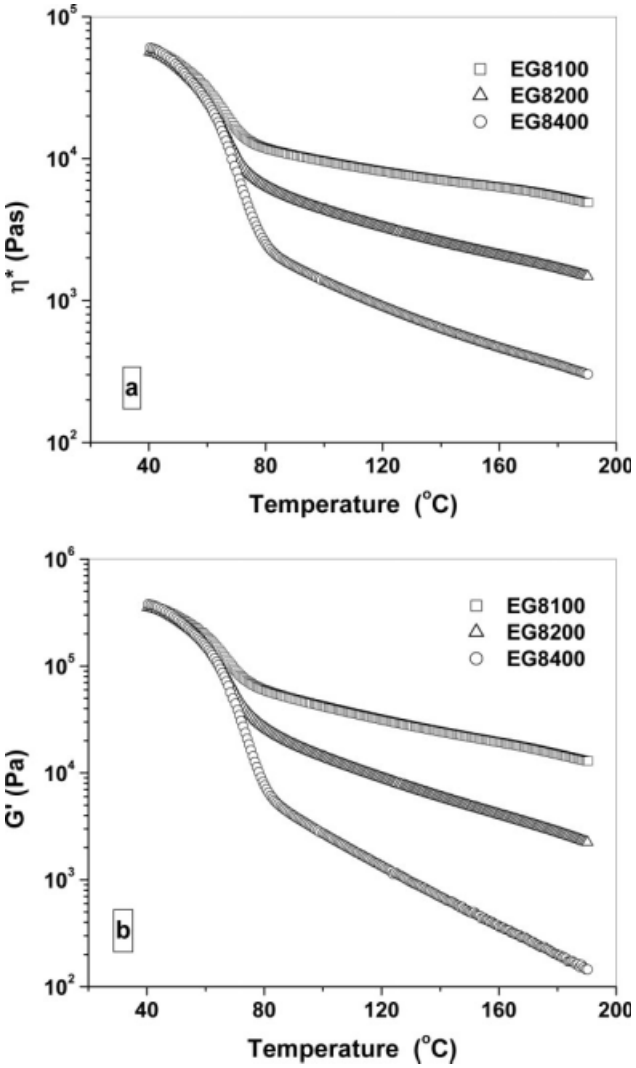

Figure 5 Temperature dependence of (a) η* and (b) G' for PEOc samples during the temperature-rising sweep process. PEOc samples were melted at 190°C for 2 min first, and the temperature was then reduced at a cooling rate of 5°C/min to 40°C. The temperature was maintained at 40°C for 1 min and then was increased at a heating rate of 5°C/min to 190°C. All dynamic temperature sweep tests were measured at a strain of 1%.

exhibited a very different expansion behavior compared to the EG8100 and EG8200 foams. Its expansion ratio tended to increase during the first 10 s and then decreased gradually afterward. This phenomenon indicated that the EG8400 foam was easier to shrink after expansion in comparison to the

TABLE II
Solubility and Diffusion Coefficients of CO_2 in the PEOc Foams at 13.8 MPa and 25°C

Sample	Solubility (wt %)	Diffusion coefficient (m^2/s)
EG8100	12.3	4.12×10^{-10}
EG8200	13.6	6.15×10^{-10}
EG8400	20.7	1.49×10^{-9}

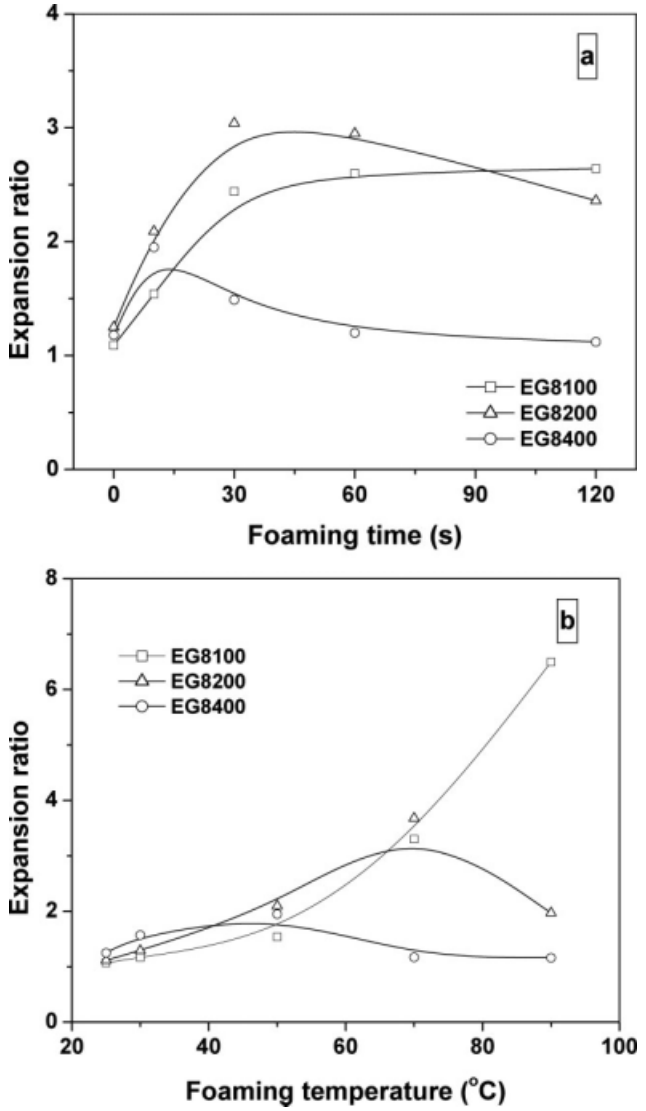

Figure 6 Expansion ratio of PEOc foams obtained (a) by foaming at 50°C for various times and (b) by foaming at 25–90°C for 10 s in a water bath. All samples were saturated at 13.8 MPa and 25°C before foaming.

EG8100 and EG8200 foams. Meanwhile, the expansion ratio of the EG8400 foam was slightly larger than that of the EG8100 foam during the first 10 s but was much lower than that of the EG8100 foam between 30 and 120 s. The effect of the foaming temperature on the expansion ratio followed a similar tendency to that of the foaming time. That is, the expansion ratio gradually increased for the EG8100 foam as the foaming temperature increased. The expansion rate began to decrease at 70°C for the EG8200 foam and at a much lower temperature of 50°C for the EG8400 foam. All of these results indicate that the foamed PEOc foams were easier to shrink with decreasing molecular weight at longer foaming times and higher foaming temperatures.

It is known that the cell growth or foam expansion process is primarily controlled by the polymer matrix modulus, melt viscoelastic properties, and gas diffusion rate.[43,44] EG8100 exhibited a higher modulus than EG8200 and EG8400. Limited cell growth caused the EG8100 foam to exhibit a lower expansion ratio when the foaming time was short, that is, 0 or 10 s, and the foaming temperature was low, that is, 25–50°C. EG8400 had high gas solubility and diffusion coefficient, which facilitated the quick expansion of the polymer foam. This was true for a short foaming time and low foaming temperature. However, with further increases in the foaming time and temperature, the expansion ratio of EG8400 tended to decrease, and only a very low expansion ratio of about 1.2 could be obtained, compared to 2.5–6.5 for the EG8100 and EG8200 foams obtained under the same foaming conditions. A possible reason was that the gas diffusion was too quick, and most of the gas diffused out of the polymer matrix at the beginning of the foam expansion process. Thus, only a very small amount of gas could be used for cell growth, although EG8400 had a higher gas solubility. EG8200 had a slightly higher gas solubility and diffusion coefficient and a lower polymer matrix modulus and melt viscosity than EG8100, which was helpful for quick foam expansion in the beginning. As shown in Figure 6(a), the EG8200 foam exhibited a high expansion ratio during foaming times of 0–60 s.

Figure 7 shows the cell morphology of the three PEOc foams obtained at foaming times of 10–120 s. For EG8100 and EG8200, all of the foamed samples had well-defined, closed-cell structures, and the cells were uniformly dispersed in the polymer matrix. The EG8400 foam also exhibited a uniform cell size distribution at foaming times of 10 and 30 s. However, with further extensions of the foaming time, the cell size distribution tended to distribute nonuniformly; a small number of large cells were observed in the polymer foam. For a foaming time of 120 s, the cells did not distribute uniformly, and unfoamed regions were seen in the polymer foam.

Figure 8 summarizes the results of the cell structure of the foamed samples as a function of foaming time, including cell size and cell density. The cell size of the EG8100 foam tended to increase with longer foaming times and then ceased when the time was longer than 30 s. The cell size of the EG8200 foam tended to increase quickly during the first 30 s and decreased slightly after a foaming time of 60 s. The maximum cell size of the EG8400 foam was obtained at a foaming time of 10 s, which was well consistent with its expansion behavior. The cell size of the EG8100 foam was lower than that of the EG8200 foam for all foaming times; this was attributed to the limited cell growth in the EG8100 foam caused by the high modulus. The cell size of the EG8400 foam was slightly larger than that of the

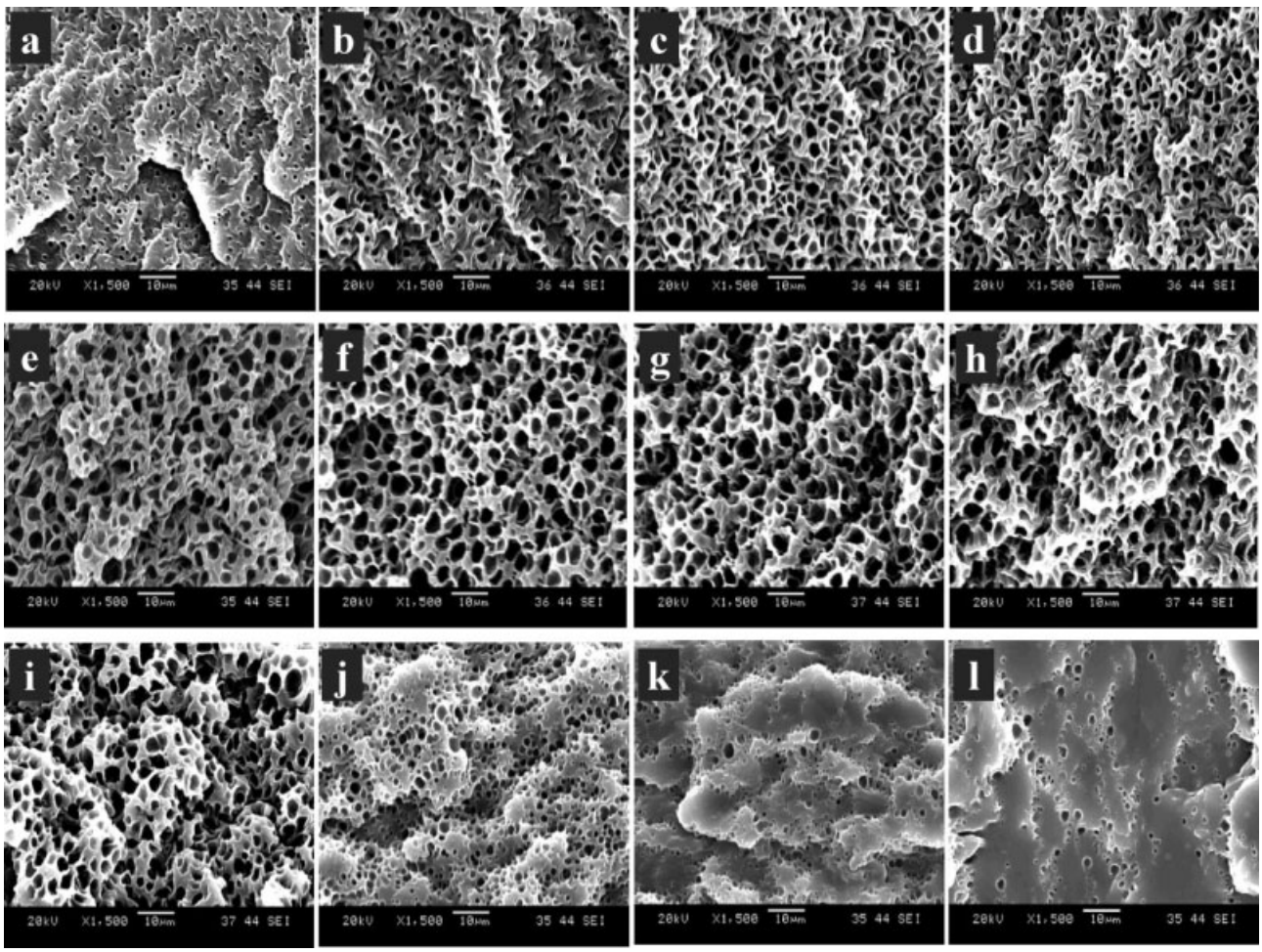

Figure 7 SEM micrographs of (a–d) EG8100, (e–h) EG8200, and (i–l) EG8400 foams saturated at 13.8 MPa and then foamed at 50°C for 10, 30, 60, and 120 s.

EG8200 foam when the samples were allowed to foam for less than or equal to 10 s; this resulted from the faster cell growth. However, with longer foaming times, the cell size tended to decrease quickly because of cell ripening.

The cell densities of the EG8100 and EG8200 foams were similar, that is, 2.8×10^{10} cells/cm^3, under the same foaming conditions. This was attributed to their similar CO_2 solubility, which resulted in similar cell nucleation during the pressure quenching. The EG8400 foam exhibited a higher cell density, that is, 7.4×10^{10} cells/cm^3, during the foaming time of 0–30 s relative to those of the EG8100 and EG8200 foams because of the higher CO_2 solubility in EG8400, as shown in Table II. However, when the foaming time was longer than 30 s, an obvious decrease in the cell density was seen in the EG8400 foam; this indicated the presence of cell ripening during a longer foaming time. The cell densities did not change in an obvious manner with the foaming time for EG8100 and EG8200 at 0–120 s and for EG8400 at 0–30 s. These results further indicate that no further cell nucleation occurred during the temperature-rising process in the water bath.

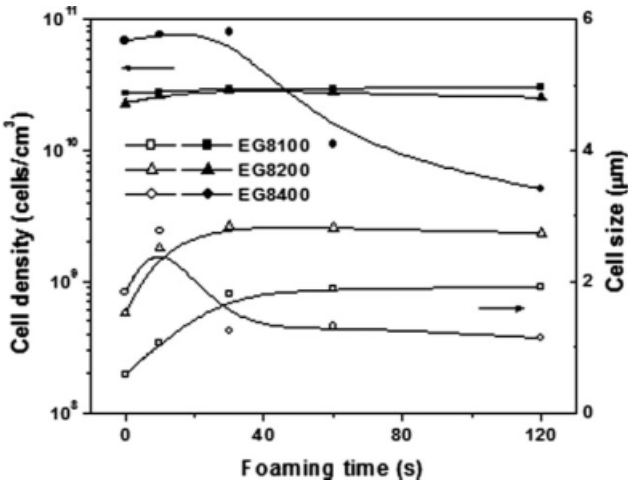

Figure 8 Cell density and cell size of three PEOc foams saturated at 13.8 MPa and foamed at 50°C for 0–120 s.

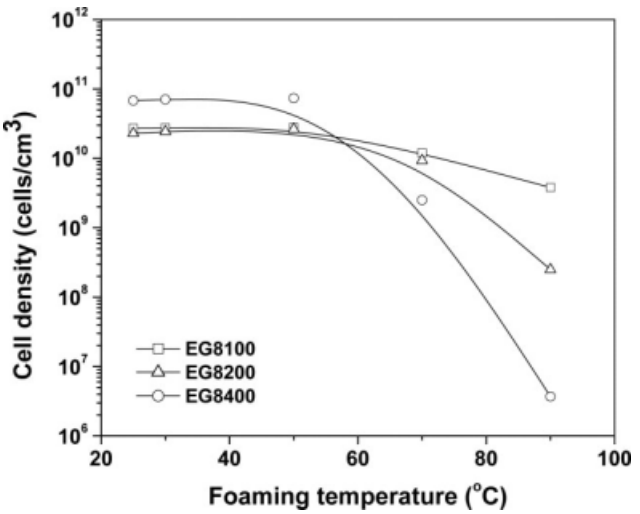

Figure 9 Cell density of the PEOc foams saturated at 13.8 MPa and foamed at 25–90°C for 10 s.

Figure 9 shows the effect of the foaming temperature on the cell density of the PEOc foams. The unchanged cell density at foaming temperatures of 25–50°C indicated that each type of foamed PEOc sample had a similar beginning point in cell nucleation. However, when the foaming temperature increased, the three PEOc foams exhibited different decreases in magnitude in cell density at 70°C, which further increased in difference at 90°C and followed this order: EG8100 < EG8200 < EG8400. The phenomenon indicated that the increase in molecular weight facilitated the suppressing of cell ripening or cell coalescence caused by the increased melt viscosity and modulus.

Just like the foaming behavior of thermoplastic polymers,[44,45] the cell densities for all three types of PEOc tended to decrease significantly with increasing foaming temperature, especially when the foaming temperature was higher than the melting point of the materials. We believe that the foaming temperature affected the cell structures through two mechanisms. First, less severe cell coalescence occurred at low foaming temperatures because of the high melt strength. In other words, the cell walls were more resistant to rupture. Second, at temperatures lower than the melting points of the PEOc samples, the existence of crystallites tended to promote the aforementioned stress-induced nucleation and, thereby, increase the cell densities. This was evident by the similar high cell densities for the foams prepared at temperatures lower than the melting points of the polymers.

The obvious cell coalescence at higher foaming temperatures was directly observed in the SEM micrographs of the PEOc foams. As shown in Figure 10, the EG8100 foam presented obvious cell coalescence near the foam surface, but uniform cell size distribution was observed in the center of foam, which was caused by the high stability of the cell structure. The cell coalescence phenomenon was observed in larger areas for the EG8200 foam, even in the center of the foam. The EG8400 foam showed significant cell coalescence in the entire polymer matrix, and a large cell was obtained in this foam, although it had a high nucleation density in the

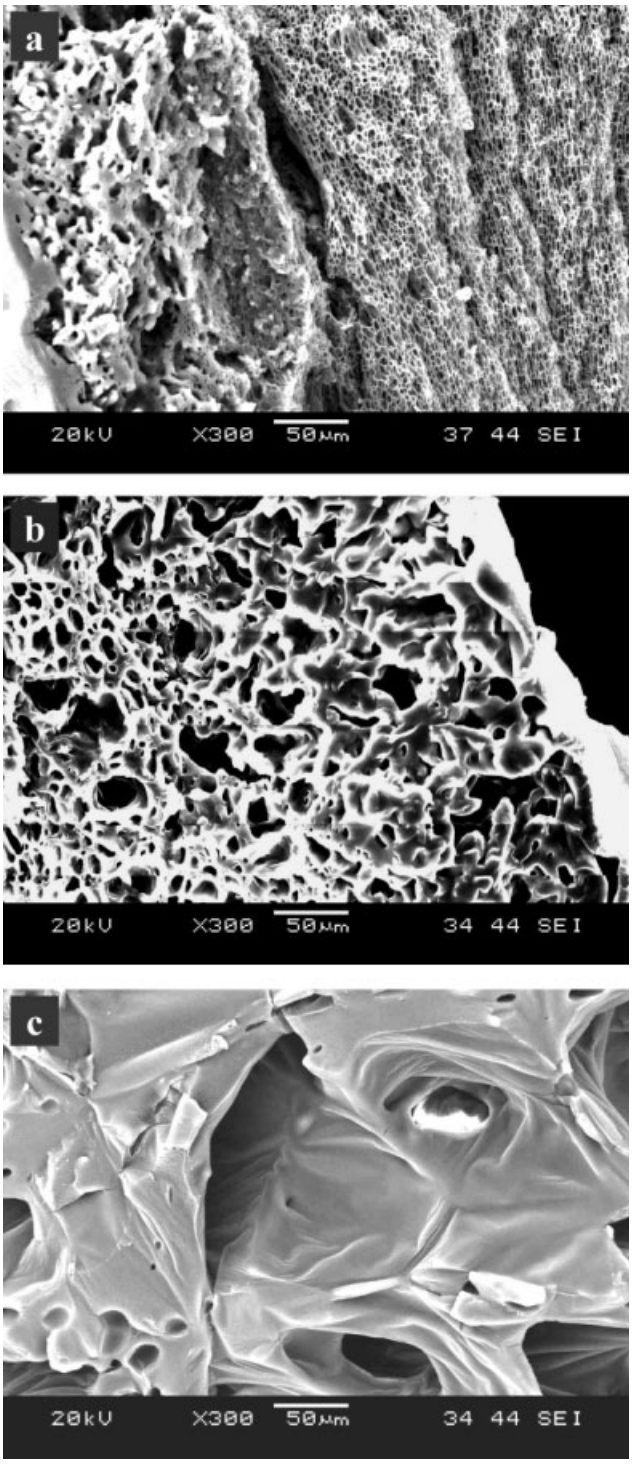

Figure 10 SEM micrographs of (a) EG8100, (b) EG8200, and (c) EG8400 foams saturated at 13.8 MPa and foamed at 90°C for 10 s.

beginning. This phenomenon further indicated the dominant effect of the melt viscoelastic properties on the cell morphology and expansion behavior of PEOc at high foaming temperatures, and the PEOc sample with a high molecular weight was more helpful for cell structure stability.

CONCLUSIONS

In this study, three types of PEOc samples with different molecular weights but the same density and similar melting behaviors were selected, and different foaming conditions were applied to determine the foaming behaviors of the TPEs and the effect of the molecular weight on the cell growth process. The results indicate that the microcellular foam of PEOc foamed with a well-defined, closed cell structure and a uniform cell size distribution was successfully prepared with CO_2 as the physical blowing agent with a batch foaming process. Microcellular PEOc foams are different from thermoplastic foams because they exhibit obvious volume shrinkage in the atmosphere, which results from the elasticity of the polymer matrix.

The polymer matrix modulus and CO_2 diffusion coefficient were important governing factors in the cell growth process. A higher molecular weight increased the polymer matrix modulus and melt viscosity and decreased the CO_2 solubility and diffusivity. EG8100 had the highest molecular weight. Its high matrix modulus limited cell growth and resulted in small cell sizes in the microcellular foam in comparison to the EG8200 and EG8400 foams with a shorter foaming time. Meanwhile, a high matrix modulus facilitated the satiability of the cell structure, and a well-defined, closed cell structure was seen at high foaming temperatures. A high CO_2 diffusion coefficient was helpful for cell growth and foam expansion. Foamed EG8400 samples with large cell sizes and a high expansion ratio were obtained at foaming times of 0 and 10 s. However, with a longer foaming time and higher foaming temperature, a high diffusion coefficient meant that less gas was used for cell growth because of the significant gas loss to the surroundings; this resulted in a smaller cell size and lower expansion ratio. EG8200 had a proper molecular weight, and the foamed samples exhibited well-defined foaming behavior.

References

1. Martini, J. E.; Waldman, F. A.; Suh, N. P. Soc Plast Eng Annu Tech Conf Tech Pap 1982, 1, 674.
2. Shen, J.; Zeng, C. C.; Lee, L. J. Polymer 2005, 46, 5218.
3. Zhai, W. T.; Yu, J.; Wu, L. C.; Ma, W. M.; He, J. S. Polymer 2006, 47, 7580.
4. Zhai, W. T.; Yu, J.; He, J. S. Polymer 2008, 49, 2430.
5. Park, C. B.; Behravesh, A. H.; Venter, R. D. Polym Eng Sci 1998, 38, 1812.
6. Xu, X.; Park, C. B.; Xu, D.; Pop-Iliev, R. Polym Eng Sci 2003, 43, 1378.
7. Gendron, R.; Daigneault, L. E. Polym Eng Sci 2003, 43, 1361.
8. Han, X. M.; Zeng, C. C.; Lee, L. J.; Koelling, K. W.; Tomasko, D. L. Polym Eng Sci 2003, 43, 1261.
9. Xu, J.; Pierick, D. Injection Molding Technol 2001, 5, 152.
10. Wong, S.; Lee, J. W. S.; Naguib, H. E.; Park, C. B. Macromol Mater Eng 2008, 293, 605.
11. Martini-Vvedensky, J. E.; Suh, N. P.; Waldman, F. A. U.S. Pat. 473,665 (1984).
12. Kumar, V.; Juntunen, R. P.; Barlow, C. Cell Polym 2000, 19, 25.
13. Collias, D. I.; Baird, D. G.; Borggreve, R. J. M. Polymer 1994, 35, 3978.
14. Collias, D. I.; Baird, D. G. Polym Eng Sci 1995, 35, 1178.
15. Collias, D. I.; Baird, D. G. Polym Eng Sci 1995, 35, 1167.
16. Shimbo, M.; Baldwin, D. F.; Suh, N. P. Polym Eng Sci 1995, 35, 1387.
17. Krause, B.; Koops, G. H.; van der Vegt, N. F. A.; Wessling, M.; Wubbenhorst, M.; van Turnhout, J. Adv Mater 2002, 14, 1041.
18. Jacobs, M. A.; Kemmere, M. F.; Keurentjes, J. T. F. Polymer 2004, 45, 7539.
19. Ito, S.; Matsunaga, K.; Tajima, M.; Yoshida, Y. J Appl Polym Sci 2007, 106, 3581.
20. Kim, S. G.; Park, C. B.; Sain, M. J Cell Plast 2008, 44, 53.
21. Walker, B. M.; Rader, C. P. Handbook of Thermoplastic Elastomers; Van Nostrand Reinhold: New York, 1998.
22. Bensason, S.; Minick, J.; Moet, A.; Chum, S.; Hiltner, A.; Baer, E. J Polym Sci Part B: Polym Phys 1996, 34, 1301.
23. Bensason, S.; Stepanov, E. V.; Chum, S.; Hiltner, A.; Baer, E. Macromolecules 1997, 30, 2436.
24. Litvinov, V. M. Macromolecules 2001, 34, 8468.
25. Muth, O.; Hirth, T.; Vogel, H. J Supercrit Fluids 2001, 19, 299.
26. Arora, K. A.; Lesser, A. J.; McCarthy, T. J. Macromolecules 1998, 31, 4614.
27. Park, C. B.; Cheung, L. K. Polym Eng Sci 1997, 37, 1.
28. Siripurapu, S.; DeSimone, J. M.; Khan, S. A.; Spontak, R. J. Adv Mater 2004, 16, 989.
29. Siripurapu, S.; Coughlan, J. A.; Spontak, R. J.; Khan, S. A. Macromolecules 2004, 37, 9872.
30. Krause, B.; Mettinkhof, R.; van der Vegt, N. F. A.; Wessling, M. Macromolecules 2001, 34, 874.
31. Leung, S. N.; Wong, A.; Park, C. B. Soc Plast Eng Annu Tech Conf Tech Pap 2009, 190.
32. Wang, L.; Leung, S. N.; Park, C. B. Soc Plast Eng Annu Tech Conf Tech Pap 2009, 997.
33. Kumar, V.; Suh, N. P. Polym Eng Sci 1990, 30, 1323.
34. Baldwin, D. F.; Park, C. B.; Suh, N. P. Polym Eng Sci 1996, 36, 1446.
35. Baldwin, D. F.; Park, C. B.; Suh, N. P. Polym Eng Sci 1996, 36, 1437.
36. Zhai, W. T.; Wang, H. Y.; Yu, J.; Dong, J. Y.; He, J. S. Polymer 2008, 49, 3146.
37. Doroudiani, S.; Park, C. B.; Korschot, M. T. Polym Eng Sci 1996, 36, 2645.
38. Lips, P. A. M.; Velthoen, I. W.; Dijkstra, P. J.; Wessling, M.; Feijen, J. Polymer 2005, 46, 9396.
39. Kumar, V.; Weller, J. E. Polym Eng Sci 1994, 34, 169.
40. Goel, S. K.; Beckman, E. J. Polym Eng Sci 1994, 34, 1148.
41. Tang, M.; Du, T. B.; Chen, Y. P. J Supercrit Fluids 2004, 28, 207.
42. Neway, B.; Westberg, Å.; Mattozzi, A.; Hedenqvist, M. S.; Giacinti Baschetti, M.; Mathoc, V. B. F.; Gedde, U. W. Polymer 2004, 45, 3913.
43. Park, C. B.; Baldwin, D. F.; Suh, N. P. Polym Eng Sci 1995, 35, 432.
44. Wang, J.; Cheng, X. G.; Yuan, M. J.; He, J. S. Polymer 2001, 42, 8265.
45. Zhai, W. T.; Wang, H. Y.; Yu, J.; Dong, J. Y.; He, J. S. Polym Eng Sci 2008, 46, 1641.